Asian Journal of Chemistry; Vol. 27, No. 1 (2015), 129-133

ASIAN JOURNAL OF CHEMISTRY

http://dx.doi.org/10.14233/ajchem.2015.16811

Density Functional Theory and Time-Dependent Density-Functional Study of Positively Charged Alkali Metal Doped Stone Whale Defective Graphene Complexes

BIN HUANG*, CUI ZHEN LI and GUO PING ZHU

Department of Materials Science and Engineering, East China Institute of Technology, Nanchang 330013, P.R. China

*Corresponding author: Tel/Fax: +86 794 8258320; E-mail: bhuang@ecit.cn

Received: 3 December 2013; *Accepted*: 26 May 2014; *Published online*: 26 December 2014; AJC-16521

The structural and electronic properties of positively charged alkali metal doped graphene and stone whale defective graphene complexes have been examined by means of density functional theory and time-dependent density-functional theories. The geometry optimization showed that Li, Na, K atom prefers to locate above the center of the hexagon ring of graphene and heptagon ring of stone whale graphene, furthermore stone whale graphene sheet occur curved. The calculated binding energies for Li, Na and K of positively charged stone whale graphene, are in the range of 0.776 to 1.104 eV and the adsorption of Na is also the weakest, which is similar to those of graphene systems. From our calculations, it can be expected that the excited and anionic states of graphene are strongly affected by Na doped, however, Na doped positively charged stone whale only causes a slightly change of electronic states of stone whale graphene, the nature of the electronic structure is hardly changed. We believe our calculations are useful to deep understanding available experimental results.

Keywords: Time-dependent density-functional, Stone whale graphene, Excitation energies, Stabilities.

INTRODUCTION

Graphene, a one-atom thick sheet of carbon atoms arranged in a honeycomb (hexagonal) lattice, forms one of the strongest in-plane bonds among all materials. Due to its unique structural, mechanical and electronical properties, graphene is an ideal materials for use in sensors, electrodes and hydrogen storage devices[1-3]. It is well known that the electronic structures of graphene can be modified by doping and adsorption, which in turn significantly change its physical and chemical properties. Nitrogen[4], boron[5] and metal atoms are the most common dopants for graphene sheets.

As for metal doping, metal doped graphene can alter its electronic properties significantly, inducing a shift of the Fermi level and shallow acceptor states of the graphene, leading to its applicability extension, such as making highly efficient sensors[6-8].

The interactions of alkali atoms and ions with carbon materials such as graphene and C_{60} are important in the development of new molecular devices[9,10]. It is widely accepted that the electronic states of graphene are drastically changed by doping of the alkali metal and ions in experiments and theoretical works. Morever, the geometrical and electronic structures of alkali metal adsorption on graphene have been investigated and potential applications of the metal-graphene systems have been proposed. Recently, many works focus on increase the binding energy of hydrogen adsorption on functionalized carbon nanotubes and graphene by Li-doping[11-16]. Especially, in the case of Li^+ doped graphene, the interaction is much important in the field of secondary rechargeable batteries[17]. As for other alkali atom doping such as Cs atom, the experimental investigations show that the total emission current of CNT increases significantly after Cs deposition and the work function of CNT reduces dramatically[18]. In theoretical, Marquez *et al.*[19] calculated the binding energy of Li^+ and hydrogen terminated graphene ($C_{32}H_{18}$) using density functional theory (DFT) method and indicated that the Li^+ ion is preferentially bound outside the graphene. On the basis of first principles calculations, Guo *et al.*[20] suggested that the ionic bonds are formed between metal atom and graphene. Besides of the stable adsorption sites and charge transfer between Li^+ ion and graphene, the diffuse path of Li^+ ion on graphene is also investigated[21]. Thus, the electronic structures at the ground states of Li^+ graphene system have been extensively studied. However, the information about excited states of other alkali atoms is sparse in recent years.

In the present contribution, ground and low-lying excited states of normal and stone whale defective graphene as well as alkali metal atom adsorption on positively charged normal and stone whale defective graphene have been investigated by means of density functional theory (DFT) method and time-dependent-density functional theory (TD-DFT) calculations

to elucidate the effect of the defect on the electronic states of graphene. In particular, we focus our attention on the Na-positively charged graphenes and stone whale graphene.

CALCULATION METHOD

In the present study, stone whale defective graphene was made by rotating a C-C bond by 90° about its center, which converts a group of four adjacent hexagonal rings into a (5,7,7,5) ring cluster, as shown in Fig. 1. The edges of graphene were terminated by hydrogen atoms, two graphene, n = 34 and 44, were examined as models of defective graphene, where n is the number of rings in stone whale defective graphene. As a comparison, normal graphene, n = 29, was also to elucidate the effect of alkali metal on the electronic states of graphene as a graphene model.

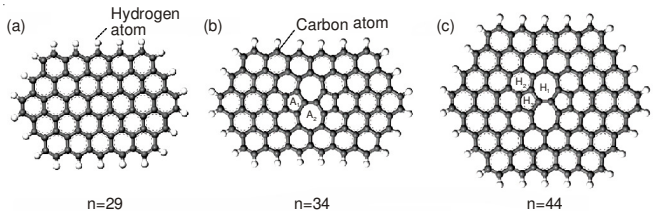

Fig. 1. Optimized structure of graphene (normal graphene) and stone-wales (SW) defects graphene at the B3LYP/6-31G(d) level. Edge region of graphene is terminated by hydrogen atom

Geometries and electronic structures of the normal graphene and stone whale -defective graphene were calculated by the B3LYP[22] functional with the 6-31G(d) basis set. For alkali metal atom adsorption on positively charged-stone whale defective graphene complex, the structures of these systems were fully optimized at the same level. The excitation energies of all systems were calculated at the time dependent (TD)-DFT[23], B3LYP/6-31G(d) level. All calculations in the present study were carried out with the Gaussian 03 program package[24].

RESULTS AND DISCUSSION

Stabilities and electronic structures of stone whale defects graphene: To test the accuracy of our model, we computed the formation energy of the stone whale defect in a graphene cluster. The stone whale defect formation energy of n = 34 were calculated to be equal to 5.58 eV, which was in reasonable agreement with the value of 6.02 eV for a planar graphene sheet predicted by Zhou and Shi using the Huckel method[25]. The optimized structure of stone whale defective graphene (n = 34 and n = 44) are given in Fig. 1, the C-C bond (A1 and A2 in Fig. 1b) are 1.462 Å and 1.332 Å, respectively. For normal graphene, the C-C bond and C-H bond lengths are calculated to be 1.420 Å and 1.088 Å, respectively. The vibrational analyses reveal that all frequencies of these optimized graphene and stone whale -defective graphene are real, showing that these carbon clusters correspond to the local energy minima on the potential energy surface, the calculated asymmetric stretching frequencies of C-C bond (A2 in Fig. 1b) is at 1872 cm^{-1} corresponding to 1610 cm^{-1} of normal graphene.

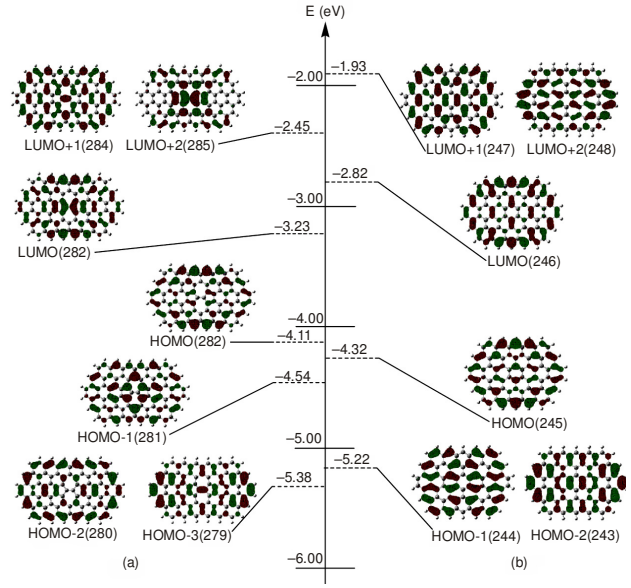

Fig. 2. Molecular orbital energies of (a) stone whale defective graphene and (b) noraml graphene calculated at the B3LYP/6-31G* level. Orbital numbers are given in parenthesis

The molecular orbitals of the stone whale defective graphene (n = 34) and normal graphene (n = 29) are depicted in Fig. 2 and the orbital energies around frontier orbitals were also shown at the B3LYP/6-31G(d) level. All the molecular orbitals as shown in Fig. 2 are widely delocalized over the stone whale defective graphene surface and normal graphene surface, respectively. HOMO-2 and HOMO-3 as well as LUMO +1 and LUMO+2 of normal graphene are doubly degenerated in energy, however, HOMO-1 and HOMO-2 as well as LUMO +1 and LUMO+2 of stone whale defective graphene are doubly degenerated in energy, indicating defects changed electronic structure of graphene. To elucidate the electronic states of graphene and stone whale defective graphene at the ground and low-lying excited states, molecular orbitals and weights of configuration state functions (CSFs) are given in Table-1. The main configurations of normal graphene for the first and

TABLE-1
EXCITATION ENERGIES AND CONFIGURATION STATE FUNCTIONS OF NORMAL GRAPHENE AND STONE WHALE (SW) DEFECTIVE GRAPHENE CALCULATED AT THE TD-DFT(B3LYP)/6-31G(D) LEVEL

State	CSF and CI vectors	E_{ex} (eV)
S1	0.597 (HOMO→LUMO)	1.487
S2	0.641 (HOMO-1→LUMO) + 0.258 (HOMO→LUMO+1)	1.878
S3	0.528 (HOMO-2→LUMO) + 0.497 (HOMO→LUMO+2)	1.920
S·1	0.678 (HOMO→LUMO) + 0.211 (HOMO→LUMO+1)	0.781
S·2	0.693 (HOMO-1→LUMO)	0.886
S·3	0.696(HOMO→LUMO+1)	1.310

(S represent states of normal graphene and S· represent states of SW defective graphene)

second excitations are Φ(HOMO-1→LUMO), Φ(HOMO→LUMO) and Φ(HOMO→LUMO+1), here, it should be noted that HOMO-1 and HOMO-2 are doubly degenerated, while LUMO+1 and LUMO+2 are also doubly degenerated. For stone whale defective graphene, while HOMO-1 is not degenerated orbital, the first state was mainly composed of Φ(HOMO → LUMO) and Φ(HOMO → LUMO+1) and second excited state was mainly composed of Φ(HOMO-1 → LUMO), which are different from those of normal graphene. These results indicate that the low-lying excited states of graphene and stone whale defective graphene are composed of the HOMO-LUMO excitations.

Structures of positively charged alkali metal doped stone whale-graphene: The geometry of positively charged Li, Na, K doped graphene (defined as Li-graphene$^+$ *etc*.) was optimized at the B3LYP/6-31G(d) level, the optimized structure is illustrated from Fig. 3a to 3c. As shown in Fig. 3, Li, Na, K atom prefers to locate above the center of the hexagon ring, the preference of alkali metal atoms at the hollow site is well known in the adsorption on the surface of CNTs and graphite. The equilibrium height of adsorbed metal atoms on graphene is the result of the electrostatic interaction. Furthermore, the height is also dependent on the atomic radius of the adatom. As the atomic radius increases, the height increases from 1.804 to 2.789 Å for positively charged Li, Na, K doped graphene, respectively. For Li-graphene$^+$, the C-C bond length around the Li atom is calculated to be 1.43 Å, which is slightly elongated by the Li doping. The calculated binding energies for Li, Na and K of positively charged systems, are in the range of 0.835 to 1.217 eV, indicating that the adsorptions of the above three atoms are all chemical adsorptions and the ionic bonds are formed between metal and graphene. Among the three adsorbates, the adsorption of Na is the weakest (0.835 eV). The relatively weaker binding of Na has also been found in the adsorption on the surface of graphite. Zhu *et al*.[26] have investigated the weaker adsorption of Na on graphite, which points out that the reason is that the single occupied molecular orbital of the Na atom is exactly at the middle point between the highest occupied molecular orbital and the lowest unoccupied molecular orbital of the graphite in the energy level.

The geometry of positively charged Li, Na, K doped stone whale defective graphene are illustrated from Fig. 3d to 3f. To find the most favorable adsorption configuration, 3 initial adsorption sites were considered in alkali metal atom adsorption on positively charged stone whale defective graphene (Fig. 1c), the most stable relaxed structure of the initial adsorption configuration H1 is shown in Fig. 3d to f, respectively. It is noted that stone whale graphene sheet occur curved in three optimized systems, which are different from positively charged alkali metal atom adsorption on graphene, it may be due to adsorption causing spin distribution on stone whale graphene. The calculated binding energies for Li, Na and K of positively charged systems (defined as Li-stone whale graphene$^+$ *etc*.), are in the range of 0.776 to 1.104 eV and the adsorption of Na is also the weakest, which is similar to those of graphene systems. In addition, as the atomic radius increases, the h from hydrogen atom to the other side hydrogen atom of stone whale graphene decreases from 21.638 to 21.597 Å. From Mulliken charge analysis as listed in Table-2, we found charge on alkali metal atom of graphene systems are slightly larger than those of stone whale defective graphene, the result indicate the electronic transport properties of the pristine graphene are different from stone whale graphene.

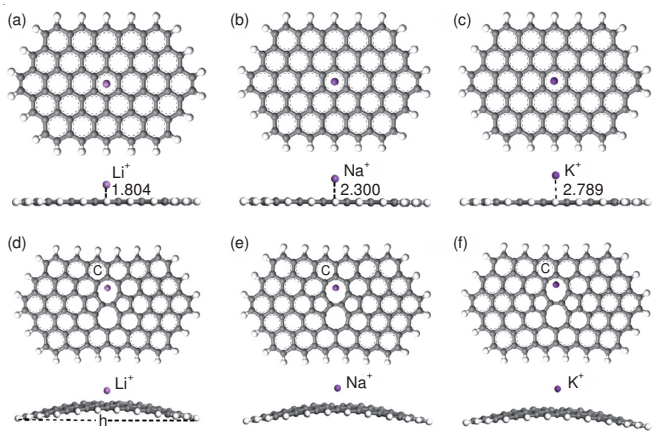

Fig. 3. Optimized geometries for the alkali metal ions-graphene complexes, (a)-(c) Li^+, Na^+ and K^+ doped-graphene, (d)-(f) Li^+, Na^+ and K^+ doped-stone whale defective graphene

Electronic structure of positively charged alkali metal doped stone whale-graphene: To elucidate the electronic features of positively charged alkali metal doped graphene and stone whale defective graphene, MO's and weights of CSF's of two containing Na systems at the excited states are analyzed. The special distributions of MO's and orbital energies around HOMO and LUMO are given in Fig. 4. For Na-graphene$^+$ (Fig. 4b), we found that HOMO, HOMO-1, LUMO are widely delocalized on graphene surface, however, LUMO+1 is localized in the Na atom, indicating Na doping inducing change of graphene electronic structures. On the other hand, for Na-stone whale graphene$^+$ (Fig. 4a), all frontier orbitals are widely delocalized on stone whale defective graphene surface. These results indicate that charged alkali metal doping on graphene causes a large change of electronic states of graphene. The excitation energies of Na-graphene$^+$

TABLE-2
CALCULATED BINDING ENERGY E_b OF THE ADSORBATE ON GRAPHENE AND STONE WHALE (SW) DEFECTIVE GRAPHENE, HEIGHT D REPRESENT DISTANCE FROM THE ADSORBATE TO GRAPHENE SURFACE, AND H REPRESENT DISTORTION OF SW DEFECTIVE GRAPHENE, Q IS CHARGE OF ALKALI METAL ATOM

Adsorbate	Graphene			SW defective graphene		
	E_b(eV)	d (Å)	Q(e)	E_b(eV)	h (Å)	Q(e)
Li	1.033	1.804	0.482	0.921	21.638	0.445
Na	0.835	2.300	0.694	0.776	21.614	0.640
K	1.217	2.789	0.880	1.104	21.597	0.858

TABLE-3
EXCITATION ENERGIES AND CONFIGURATION STATE FUNCTIONS OF Na DOPED NORMAL GRAPHENE$^+$ AND Na DOPED SW DEFECTIVE GRAPHENE$^+$ CALCULATED AT THE TD-DFT(B3LYP)/6-31G(D) LEVEL

State	CSF and CI vectors	E_{ex} (eV)
S1	0.697 (HOMO→LUMO)	1.331
S2	0.641 (HOMO-1→LUMO)+ 0.258 (HOMO→LUMO+1)	1.482
S3	0.638 (HOMO-2→LUMO)+ 0.271 (HOMO→LUMO+2)	1.804
S·1	0.680 (HOMO→LUMO)+ 0.221 (HOMO→LUMO+1)	0.697
S·2	0.693 (HOMO-1→LUMO)	0.859
S·3	0.696(HOMO→LUMO+1)	1.193

(S represent states of normal graphene and S· represent states of stone whale defective graphene)

and stone whale graphene$^+$ are given in Table-3. It was found that the first and second excitation energies of the Na-stone whale graphene$^+$ were calculated to be 0.697 and 0.859 eV, respectively, indicating that the excitation energies are slightly red shifted compared to those of stone whale defective graphene. For Na doped graphene$^+$, due to LUMO+1 localization in the Na atom, it was found that the second excitation were significantly higher than those of stone whale defecitve graphene.

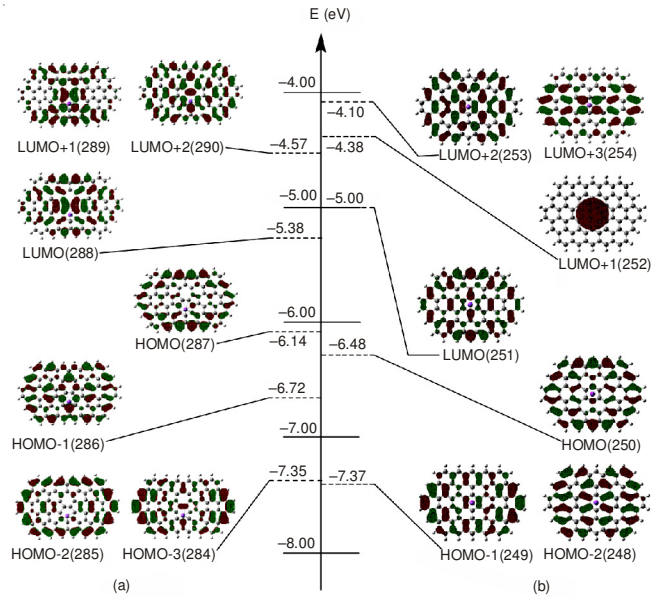

Fig. 4. Molecular orbital energies of (a) Na$^+$ doped-stone whale graphene and (b) Na$^+$ doped-graphene calculated at the B3LYP/6-31G* level. Orbital numbers are given in parenthesis

The coefficients of CSFs in the Na-graphene$^+$ and Na-stone whale graphene$^+$ are summarized in Table-3. For Na-stone whale graphene$^+$, the first excited state was mainly composed of two CSFs, Φ(HOMO→LUMO) and Φ(HOMO →LUMO+1), while the coefficients of CSFs for the former and the latter were calculated to be 0.680 and 0.221, respectively. The second excited state is mainly composed of Φ(HOMO→LUMO+1) with the coefficient of 0.693. From the above analysis, the orbital images of first and second excitations as shown in Fig. 4a are the same as those of stone whale graphene, these results indicate that Na-stone whale graphene$^+$ causes a slightly change of electronic states of stone whale graphene, the nature of the electronic structure is hardly changed. For Na-graphene$^+$, the first excited state is mainly composed of Φ(HOMO→LUMO) with the coefficient of 0.697. The second excited state was mainly composed of two CSFs, Φ(HOMO-1→LUMO) and Φ(HOMO→LUMO+1), while the coefficients of CSFs for the former and the latter were calculated to be 0.641 and 0.258, respectively. From our calculations, it can be expected that the excited and anionic states of graphene are strongly affected by Na doped. In Na-graphene$^+$ system, *s*-orbital of Na contaminates to LUMO+1 orbital, as shown in Fig. 4b. This orbital contamination causes the spectrum shift, the magnitude of contamination is significantly large, so that the second excitation is large red shift. This feature is much different from the Na-stone whale graphene$^+$ in which both frontier orbitals are delocalized on the graphene surface.

Conclusion

Quantum chemical calculations were performed to study the structural and electronic properties of positively charged alkali metal doped graphene and stone whale defective graphene complexes. The calculations were carried out at the density functional theory (DFT) and time-dependent density-functional (TD-DFT) theories. The geometry optimization showed that Li, Na, K atom prefers to locate above the center of the hexagon ring of graphene and heptagon ring of stone whale graphene, furthermore stone whale graphene sheet occur curved. The calculated binding energies for Li, Na and K of positively charged stone whale graphene, are in the range of 0.776 to 1.104 eV and the adsorption of Na is the weakest, which is similar to those of graphene systems. From our calculations, it can be expected that the excited and anionic states of graphene are strongly affected by Na doped. However, Na doped positively charged stone whale only causes a slightly change of electronic states of stone whale graphene, the nature of the electronic structure is hardly changed. Present results provide a basis for further experimental and theoretical exploration of the ground and excited electronic states of doped graphene and defective graphene.

ACKNOWLEDGEMENTS

This work was supported by Nature Science Foundation of Jiangxi Province (20114BAB213010) and the Foundation of Jiangxi Educational Committee (No. GJJ11487, GJJ14485).

REFERENCES

1. A.K. Geim, *Science*, **324**, 1530 (2009).
2. C.N.R. Rao, A.K. Sood, K.S. Subrahmanyam and A. Govindaraj, *Angew. Chem. Int. Ed.*, **48**, 7752 (2009).
3. K.R. Ratinac, W. Yang, S.P. Ringer and F. Braet, *Environ. Sci. Technol.*, **44**, 1167 (2010).

4. S.S. Yu, W.T. Zheng, Q.B. Wen and Q. Jiang, *Carbon*, **46**, 537 (2008).
5. S.S. Yu and W.T. Zheng, *Nanoscale*, **2**, 1069 (2010).
6. Y. Qian, S.B. Lu and F.L. Gao, *Mater. Lett*., **65**, 56 (2011).
7. E.H. Song, Z. Wen and Q. Jiang, *J. Phys. Chem. C*, **115**, 3678 (2011).
8. S. Wannakao, T. Nongnual, P. Khongpracha, T. Maihom and J. Limtrakul, *J. Phys. Chem. C*, **116**, 16992 (2012).
9. M. Inagaki, H. Tachikawa, T. Nakahashi, H. Konno and Y. Hishiyama, *Carbon*, **36**, 1021 (1998).
10. H. Konno, K. Shiba, H. Tachikawa, T. Nakahashi, H. Oka and M. Inagaki, *Synth. Met*., **125**, 189 (2001).
11. W.Q. Deng, X. Xu and W.A. Goddard, *Phys. Rev. Lett.*, **92**, 166103 (2004).
12. H. Tachikawa, Y. Nagoya and T. Fukuzumi, *J. Power Sources*, **195**, 6148 (2010).
13. J.H. Cho and C.R. Park, *Catal. Today*, **120**, 407 (2007).
14. L. Chen, Y.M. Zhang, N. Koratkar, P. Jena and S.K. Nayak, *Phys. Rev. B*, **77**, 033405 (2008).
15. I. Cabria, M.J. Lopez and J.A. Alonso, *J. Chem. Phys*., **123**, 204721 (2005).
16. L. Qiao, C.Q. Qu, H.Z. Zhang, S.S. Yu, X.Y. Hu, X.M. Zhang, D.M. Bi, Q. Jiang and W.T. Zheng, *Diamond Rel. Mater.*, **19**, 1377 (2010).
17. D. Pan, S. Wang, B. Zhao, M. Wu, H. Zhang, Y. Wang and Z. Jiao, *Chem. Mater*., **21**, 3136 (2009).
18. X. Duan, B. Akdim and R. Pachter,, *Appl. Surf. Sci*., **243**, 11 (2005).
19. A. Marquez, A. Vargas and P.B. Balbuena, *J. Electrochem. Soc*., **145**, 3328 (1998).
20. H. Tachikawa and A. Shimizu, *J. Phys. Chem. B*, **110**, 20445 (2006).
21. J. Zheng, Z. Ren, P. Guo, L. Fang and J. Fan, *Appl. Surf. Sci*., **258**, 1651 (2011).
22. A.D. Becke, *J. Chem. Phys*., **84**, 4524 (1986).
23. (a) R.E. Stratmann, G.E. Scuseria and M.J. Frisch, *J. Chem. Phys*., **109**, 8218 (1998).; (b) R. Bauernschmitt and R. Ahlrichs, *Chem. Phys. Lett*., **256**, 454 (1996).; (c) M.E. Casida, C. Jamorski, K.C. Casida and D.R. Salahub, *J. Chem. Phys*., **108**, 4439 (1998).
24. M.J. Frisch, G.W. Trucks, H.B. Schlegel, G.E. Scuseria, M.A. Robb, J.R. Cheeseman, J.J.A. Montgomery, T. Vreven, K.N. Kudin, J.C. Burant, J.M. Millam, S.S. Iyengar, J. Tomasi, V. Barone, B. Mennucci, M. Cossi, G. Scalmani, N. Rega, G.A. Petersson, H. Nakatsuji, M. Hada, M. Ehara, K. Toyota, R. Fukuda, J. Hasegawa, M. Ishida, T. Nakajima, Y. Honda, O. Kitao, H. Nakai, M. Klene, X. Li, J.E. Knox, H.P. Hratchian, J.B. Cross, V. Bakken, C. Adamo, J. Jaramillo, R. Gomperts, R.E. Stratmann, O. Yazyev, A.J. Austin, R. Cammi, C. Pomelli, J.W. Ochterski, P.Y. Ayala, K. Morokuma, G.A. Voth, P. Salvador, J.J. Dannenberg, V.G. Zakrzewski, S. Dapprich, A.D. Daniels, M.C. Strain, O. Farkas, D.K. Malick, A.D. Rabuck, K. Raghavachari, J.B. Foresman, J.V. Ortiz, Q. Cui, A.G. Baboul, S. Clifford, J. Cioslowski, B.B. Stefanov, G. Liu, A. Liashenko, P. Piskorz, I. Komaromi, R.L. Martin, D.J. Fox, T. Keith, M.A. Al-Laham, C.Y. Peng, A. Nanayakkara, M. Challacombe, P.M.W. Gill, B. Johnson, W. Chen, M.W. Wong, C. Gonzalez and J.A. Pople, Gaussian 03, Revision C.02, Gaussian, Inc., Wallingford CT (2004).
25. L.G. Zhou and S.-Q. Shi, *Appl. Phys. Lett*., **83**, 1222 (2003).
26. Z.H. Zhu and G.Q. Lu, *Langmuir*, **20**, 10751 (2004).